
Applied Vacuum Electrodynamics

The Mechanical Substrate of Physics

Grant Lindblom

Abstract

Modern physics models the universe as a passive stage governed by abstract laws. Applied Vacuum Electrodynamics (AVE) redefines the universe as an active physical machine: a Discrete Amorphous Manifold (M_A) governed by hardware specifications. By postulating two fundamental limits—the Lattice Pitch (l_0) and Breakdown Voltage (V_0)—we derive the "constants" of nature not as fixed scalars, but as the emergent operating limits of the substrate.

From these axioms, we derive:

- **Quantum Mechanics:** The bandwidth limitation of a discrete signaling network (Nyquist-Shannon).
- **Gravity:** The refractive gradient of the lattice density ($n(r)$), derived via the Elastic Green's Function.
- **Matter:** Topological solitons (Knots) where the fine-structure constant (α^{-1}) emerges from the holomorphic impedance of the trefoil geometry ($4\pi^3 + \pi^2 + \pi$).
- **The Dark Sector:** Dark Energy is resolved as the Latent Heat of lattice crystallization, and Dark Matter as the hydrodynamic viscosity of the vacuum fluid.

This framework is strictly falsifiable. We propose the **Rotational Lattice Viscosity Experiment (RLVE)**, which predicts a density-dependent phase shift ($\Psi > 5$) that contradicts General Relativity, providing a decisive "Kill Switch" for the theory.

VACUUM ENGINEERING PRESS

Applied Vacuum Engineering: The Mechanical Substrate of Physics
Copyright © 2026 Grant Lindblom

This document is a technical specification. All constants derived herein are subject to the hardware limitations of the local vacuum manifold.

Contents

Nomenclature and Fundamental Constants	vi
Glossary and Acronyms	viii
I The Hardware Layer: Vacuum Constitutive Properties	1
1 The Hardware Layer	2
1.1 The Constitutive Substrate	2
1.2 Node Geometry and Topological Helicity	2
1.2.1 The Chiral Bias Equation (CBE)	3
1.3 Hardware Saturation and the Origin of Mass	3
1.4 Permeability and Permittivity as Bulk Moduli	3
2 The Signal Layer	5
2.1 The Vacuum Dispersion Relation	5
2.1.1 Derivation from Discrete Kirchhoff Laws	5
2.1.2 Relativistic Scaling as Bandwidth Limiting	6
2.2 The Origin of Inertia as Back-EMF	6
2.3 Gravity as Metric Refraction	7
2.4 Time Dilation as Lattice Latency	7
2.5 Exercises	7
II The Quantum Layer: Defects and Chiral Exclusion	8
3 The Quantum Layer	9
3.1 Introduction: The End of Probabilistic Abstraction	9
3.2 Topological Helicity as Quantized Spin	9
3.3 The Chiral Exclusion Principle	10
3.3.1 Impedance Clamping and Parity	10
3.4 Determinism and the Pilot Wave	10
3.5 The Nyquist-Heisenberg Resolution	11
3.6 Exercises	11
4 The Topological Layer	12
4.1 Introduction: The Periodic Table of Knots	12

4.2	Helicity as Charge	12
4.3	Modeling the Electron and Proton	13
4.3.1	The Electron: The Simple Vortex	13
4.3.2	The Proton: The Trefoil Knot	13
4.4	Topological Stability and Decay	13
4.5	Exercises	14
4.6	Transition to the Weak Layer	14
5	The Weak Interaction	15
5.1	Introduction: Beyond the Boson	15
5.2	The Inverse Resonance Scaling Law	15
5.3	Chiral Clamping and the Weinberg Angle	16
5.3.1	The Mechanical Weinberg Angle	16
5.4	Beta Decay as a Hardware Discharge	16
5.5	Simulation: Emergent Clamping	17
5.6	Exercises	17
III	Macroscale Dynamics and Engineering	18
6	Cosmic Evolution	19
6.1	The Quench Hypothesis	19
6.2	The Impedance Evolution Equation	19
6.3	Variable Speed of Light and the Horizon Problem	20
6.4	Metric Aging and Radioactive Decay	20
6.5	The Stability of the Fine Structure Constant (α)	20
6.6	Exercises	21
7	Macroscale Dynamics	22
7.1	Introduction: The Dark Matter Fallacy	22
7.2	The Mass-Loading of the Manifold	22
7.2.1	The Radial Impedance Function	22
7.3	Falsification: The Bullet Cluster and Lattice Memory	23
7.4	The Tully-Fisher Relation as an Impedance Law	23
7.5	Exercises	24
8	The Engineering Layer	25
8.1	The Principle of Local Impedance Control	25
8.2	Metric Refraction: The Non-Geometric Warp	25
8.2.1	The Lattice Stress Coefficient (σ)	26
8.3	Topological Shorts and Zero-Point Extraction	26
8.4	Metric Shielding and Inertia Nullification	26
8.5	Exercises	26

IV Falsifiability and Verification	28
9 Falsifiability	29
9.1 Introduction: The Requirement of Vulnerability	29
9.2 The Neutrino Parity Kill-Switch	29
9.3 The Spectroscopic Invariance Test	30
9.3.1 The Fine Structure Constant (α)	30
9.4 The GZK Cutoff as a Hardware Nyquist Limit	30
9.5 Engineering Layer: The Metric Null-Result	30
9.6 The Bullet Cluster and Lattice Memory	31
9.7 Summary of Falsification Thresholds	31
A Mathematical Proofs and Formalism	32
A.1 A.1 The Discrete-to-Continuum Limit (Kirchhoff)	32
A.2 A.2 The Madelung Internal Pressure (Q)	33
A.3 A.3 Impedance Clamping and Parity Violation	33
B Simulation Manifest and Codebase	34
C Simulation Code Repository	37
C.1 C.1 Introduction	37
C.2 C.2 Core Code: Metric Lensing	37
C.3 C.3 Core Code: The Cosmic Quench	38
D The Rosetta Stone	44
D.1 D.1 The Mapping Table	44
D.2 D.2 Key Descriptive Definitions	46

Preface: The Hardware Perspective

Traditional physics asks "What are the laws?" Engineering asks "What are the specs?" This book is an attempt to answer the second question. By treating the universe not as a mathematical abstraction but as a physical machine, we find that the "laws" are simply the operating limits of the hardware.

Part I

The Constitutive Substrate

Chapter 1

Discrete Amorphous Manifold: Topology of the Substrate

1.1 The Fundamental Axioms of Vacuum Engineering

To eliminate circular definitions and reduce the universe to a mechanical substrate, the **Applied Vacuum Electrodynamics (AVE)** framework rests entirely on six fundamental hardware axioms. All other physics are derived as emergent behaviors of these limits.

- **Axiom I: The Discrete Substrate Limit (l_0)**. The universe is not a continuous geometry, but a discrete, amorphous transmission network. The mean edge length between nodes is the fundamental **Lattice Pitch** (l_0). This is an independent hardware primitive, empirically bounded by high-energy cosmic ray cutoffs (GZK limit) to approximately 1.6×10^{-35} m. *Calibration Note:* Matching the derived Planck scale sets $l_0 \sim 10^{-35}$ m (order-of-magnitude). In AVE l_0 is a primary input parameter of the mesh, not a secondary derivative of constants G and \hbar .
- **Axiom II: The Constitutive Moduli (μ_0, ϵ_0)**. Each node acts as a reactive circuit element possessing Inductance Density (μ_0 , resistance to flux displacement) and Capacitance Density (ϵ_0 , elastic charge storage).
- **Axiom III: The Global Slew Rate (c)**. The speed of light is the maximum signal propagation slew rate of the discrete network: $c = 1/\sqrt{\mu_0\epsilon_0}$.
- **Axiom IV: The Saturable Dielectric Condition**. Near breakdown ($U \approx U_{sat}$), the capacitance clamps to a maximum saturation value, localizing energy as stable topological knots (Matter).
- **Axiom V: The Generative Manifold (H_0)**. The continuous quantum potential underlying the graph constantly crystallizes into new discrete nodes at the Genesis Rate ($H_0 \approx 2.3 \times 10^{-18}$ Hz).
- **Axiom VI: The Fundamental Breakdown Voltage (V_0)**. The absolute maximum potential difference a single node can sustain before the lattice bonds rupture is an empirically anchored hardware limit: $V_0 \approx 1.04 \times 10^{27}$ V.

1.2 The Amorphous Manifold

The foundational postulate of the AVE framework is that the physical universe is a Discrete Amorphous Manifold (M_A). Let P be a set of stochastic points distributed in a topological volume V . The physical manifold M_A is defined as the Delaunay Triangulation of P .

Definition 1.1 (The Amorphous Manifold) *Let \mathcal{P} be a set of stochastic points distributed in a topological volume \mathcal{V} with mean density ρ_{node} . The physical manifold M_A is defined as the **Delaunay Triangulation** of \mathcal{P} .*

- **Nodes (V):** The active processing elements of the vacuum.
- **Edges (E):** The flux transmission lines connecting nearest neighbors.
- **Cells (Φ):** The Voronoi cells representing the effective volume of each node.

1.2.1 The Fundamental Lattice Pitch (l_0)

Just as a digital image has a pixel size, the vacuum has a fundamental granularity. We define the **Lattice Pitch** (l_0) as the mean edge length of the graph:

$$l_0 = \langle |e_{ij}| \rangle \approx 1.6 \times 10^{-35} \text{ m} \quad (1.1)$$

This length scale is the physical separation between the inductive nodes of the substrate. It imposes a "Hardware Cutoff" frequency ($\omega_{max} \approx c/l_0$) on all physical signals, naturally preventing ultraviolet divergences.

Calibration Note: Matching the derived Planck scale sets $l_0 \sim 10^{-35} \text{ m}$ (order-of-magnitude). In AVE l_0 is a primary input parameter of the mesh, not a secondary derivative of constants G and \hbar .

1.2.2 Isotropy via Stochasticity: The Rifled Vacuum

A common critique of discrete spacetime models is the "Manhattan Distance" problem. On a regular cubic grid, diagonal movement is mathematically longer than cardinal movement ($\sqrt{2}$ vs 1), which violates Lorentz Invariance and would cause the speed of light to vary with direction.

The M_A framework evades this by requiring the lattice to be **Amorphous** (Random) rather than Crystalline.

Theorem 1.2 (Isotropic Averaging)

For a Delaunay graph generated from a stochastic Poisson distribution, the effective path length approaches rotational invariance at macroscopic scales ($L \gg l_0$).

$$\lim_{N \rightarrow \infty} \mathcal{L}f(x) \approx \nabla^2 f(x) \quad (1.2)$$

While the photon performs a random walk at the micro-scale (The Jagged Path), the Graph Laplacian (\mathcal{L}) converges to the continuous Laplace-Beltrami operator (∇^2) at the macro-scale. The vacuum looks smooth to us for the same reason a sandy beach looks smooth

from an airplane: the grains (lattice pitch l_0) are stochastic, and the signal is gyroscopically stabilized.

Physical Result: Light travels at the same speed in every direction. The vacuum looks smooth to us for the same reason a sandy beach looks smooth from an airplane: the grains (lattice pitch l_0) are stochastic and infinitesimally small.

1.2.3 Connectivity Analysis

Unlike a crystalline lattice with a fixed coordination number (e.g., 6 for cubic, 12 for FCC), the vacuum substrate possesses a statistical distribution of connectivity. Monte Carlo analysis of $N = 10,000$ nodes yields a mean coordination number:

$$\langle k \rangle \approx 15.54 \quad (1.3)$$

This high degree of connectivity ensures that the vacuum is "Over-Braced," providing the extreme mechanical stiffness required to support the propagation of transverse waves (light) at c while minimizing dispersive loss.

1.3 The Moduli of the Void

In standard physics, μ_0 and ϵ_0 are treated as mere scaling constants for units. In Vacuum Engineering, they are the **Constitutive Moduli** of the mechanical substrate.

1.3.1 Magnetic Permeability (μ_0) as Density

The magnetic constant μ_0 represents the **Inductive Inertia** of the lattice nodes. It quantifies the resistance of the vacuum to a changing flux current (dI/dt).

$$\mu_0 \approx 1.256 \times 10^{-6} \text{ H/m} \quad (1.4)$$

Mechanically, this is analogous to the fluid density (ρ) in hydrodynamics. It determines how "heavy" the vacuum is. A high μ_0 means the lattice is chemically sluggish; it resists changes in state. This inductive lag is the physical origin of **Inertial Mass**.

1.3.2 Electric Permittivity (ϵ_0) as Elasticity

The electric constant ϵ_0 represents the **Capacitive Compliance** of the lattice edges. It quantifies how much the vacuum can be polarized (stretched) by an electric field before snapping back.

$$\epsilon_0 \approx 8.854 \times 10^{-12} \text{ F/m} \quad (1.5)$$

Mechanically, this is the inverse of the Bulk Modulus (K). It determines how "stiff" the vacuum is. A low ϵ_0 implies a stiff lattice that transmits force at speeds approaching the lattice mode speed limit (c).

1.3.3 Characteristic Impedance (Z_0)

The ratio of these two moduli defines the **Characteristic Impedance** of the universe:

$$Z_0 = \sqrt{\frac{\mu_0}{\epsilon_0}} \approx 376.73 \Omega \quad (1.6)$$

This is the "acoustic impedance" of the vacuum. It dictates the efficiency of energy transfer. The fact that Z_0 is finite (and not zero) is the only reason electromagnetic waves can propagate at all.

1.4 The Global Slew Rate (c)

The speed of light is not an arbitrary speed limit imposed by traffic laws; it is the **Global Slew Rate** of the hardware.

1.4.1 Derivation from Moduli

In any transmission line, the propagation velocity is determined strictly by the distributed inductance and capacitance. Using the moduli defined in Section ??:

$$c = \frac{1}{\sqrt{\mu_0 \epsilon_0}} \quad (1.7)$$

Substituting the measured values:

$$c = \frac{1}{\sqrt{(1.256 \times 10^{-6})(8.854 \times 10^{-12})}} \approx 299,792,458 \text{ m/s} \quad (1.8)$$

This derivation proves that c is not a fundamental constant itself, but an emergent property of the substrate's stiffness and density.

1.4.2 The Bandwidth Limit

Physically, c represents the maximum rate at which a lattice node can update its internal state vector. It is the **Clock Speed** of the manifold.

- **Massless Particles:** Travel at the slew rate because they have no inductive core to charge up.
- **Massive Particles:** Travel slower than c because they must constantly "charge" and "discharge" the local vacuum inductance as they move (see Chapter 3).

1.5 Dielectric Saturation Limit

Every physical material has a breakdown voltage. The vacuum is no exception. We define the **Breakdown Voltage** (V_0) as the saturation limit of the lattice.

1.5.1 The Schwinger Limit

Standard QED predicts that at an electric field strength of $E_{crit} \approx 1.32 \times 10^{18}$ V/m, the vacuum "boils," spontaneously generating electron-positron pairs. In Vacuum Engineering, this is the point where the capacitive edges of the graph (E) rupture.

1.5.2 Non-Linear Response

Below this limit, the vacuum acts as a linear medium (Hooke's Law). Near this limit, the stress-strain curve becomes non-linear.

$$D = \epsilon_0 E + \chi^{(3)} E^3 + \dots \quad (1.9)$$

This non-linearity is crucial for:

1. **Particle Genesis:** Creating stable topological knots (Matter).
2. **Black Holes:** Regions where the lattice is stressed to maximal density.

We postulate that the **Saturation Energy** (E_{sat}) is simply the total energy storage capacity of a single lattice cell before dielectric breakdown occurs.

1.6 Theoretical Constraints on Fundamental Constants

Standard physics treats G and \hbar as unexplained, fundamental scalars. In the AVE framework, we propose they are strictly emergent scaling factors derived from the two fundamental hardware primitives: Lattice Pitch (l_0) and Vacuum Breakdown Voltage (V_0). We derive them here without invoking circular Planck-unit definitions. In particular, Planck-length identities (e.g. $l_P = \sqrt{\hbar G/c^3}$) are used only as *post-hoc consistency checks* and never appear inside the derivations.

1.6.1 Independent Hardware Primitives and Derived Scales

A recurring failure mode of “emergent constants” models is accidental circularity: one introduces a parameter that is secretly defined using the very constants one claims to derive. To avoid this, we separate *independent hardware primitives* (axioms) from *derived scales* (consequences), and from *calibration* (matching to empirically measured values).

The Nodal Breakdown Voltage (V_0)

To avoid circular definitions involving \hbar , we define the Breakdown Voltage V_0 strictly as the energy cost of rupturing a single lattice node’s connectivity. While the Schwinger Limit ($E_{crit} \approx 10^{18}$ V/m) represents the onset of pair-production (soft breakdown), V_0 represents the **Hard Topological Rupture** of the manifold (Singularity Formation).

We postulate V_0 as the potential required to displace a node by one full lattice pitch l_0 against the vacuum’s bulk modulus. We define the **Nodal Charge Capacity** (Q_{node}) as the maximum topological flux a single node can sustain:

$$V_0 \equiv \sqrt{\frac{1}{4\pi\epsilon_0} \frac{Q_{node}^2}{l_0}} \approx 1.04 \times 10^{27} \text{ V} \quad (1.10)$$

Note on Circularity: Here, Q_{node} is the hardware limit of the manifold. While numerical calibration reveals that $Q_{node} \approx q_{Planck}$, we treat Q_{node} as the independent geometric capacity of the Delaunay mesh, not as a derivative of \hbar . This anchors V_0 to the *geometric limit* where the electrostatic potential energy of a single node equals the mass-energy of the entire observable universe's horizon.

Primitive (Axiomatic) Hardware Parameters

We postulate the vacuum substrate as a discrete manifold (M_A) with two independent microphysical hardware primitives:

1. **Lattice pitch** l_0 (a true microscopic length scale of the substrate).
2. **Breakdown voltage** V_0 (maximum node-to-node potential sustainable before dielectric rupture / pair-production onset).

No Planck-unit identities are assumed in defining l_0 or V_0 . In addition, we use the *measured* electromagnetic moduli (ϵ_0, μ_0) only to set the low-energy continuum normalization of the substrate (i.e. the IR limit must reproduce standard electrodynamics).

In particular, the Global Slew Rate:

$$c \equiv \frac{1}{\sqrt{\mu_0\epsilon_0}} \quad (1.11)$$

is treated as an emergent *IR* propagation speed fixed by the observed moduli.

Geometric Reduction Factors (Order-Unity)

A discrete amorphous lattice requires geometric coarse-graining factors that are generically $\mathcal{O}(1)$ and encode coordination number / packing geometry. We therefore write the effective node capacitance and inductive energy partition as:

$$C_{node} \equiv \kappa_C \epsilon_0 l_0, \quad E_{sat} \equiv \kappa_E C_{node} V_0^2, \quad (1.12)$$

where $\kappa_C, \kappa_E \sim \mathcal{O}(1)$ absorb non-universal microscopic geometry. (For a simple LC node with equipartition between electric and magnetic storage, $\kappa_E = 1$ is a natural starting point.)

We also define the fundamental substrate clock (update time) as:

$$t_{\text{tick}} \equiv \frac{l_0}{c}. \quad (1.13)$$

This is not a relativistic axiom; it is the microscopic update time of a discretized manifold.

Derived Action Scale (Quantum of Action)

We define the maximum *action capacity* of a single node as:

$$\hbar_{\text{AVE}} \equiv E_{\text{sat}} t_{\text{tick}} = (\kappa_E C_{\text{node}} V_0^2) \left(\frac{l_0}{c} \right) = \frac{\kappa_E \kappa_C \epsilon_0 l_0^2 V_0^2}{c}. \quad (1.14)$$

Equation (??) is a *non-circular* derived relationship: it depends only on the primitives (l_0, V_0) , the observed IR modulus ϵ_0 , and an $\mathcal{O}(1)$ geometric factor.

Calibration vs. derivation. If one *chooses* $(l_0, V_0, \kappa_C \kappa_E)$ such that \hbar_{AVE} matches the empirical \hbar , then the model has successfully *calibrated* its microscopic limits to the observed quantum of action. This is not a tautology: no Planck identity is used to enforce the result. It is a falsifiable constraint on the product $\kappa_C \kappa_E l_0^2 V_0^2$.

Derived Gravitational Coupling as Mechanical Compliance

We next define a mechanical stiffness scale from the statement: “the maximum transmissible mechanical work per lattice pitch is E_{sat} ”. This implies a yield force scale:

$$F_{\text{yield}} \equiv \frac{E_{\text{sat}}}{l_0}. \quad (1.15)$$

To connect this to macroscopic gravity, we introduce a *definition* of the substrate stiffness-to-curvature conversion by equating a universal stiffness scale to the familiar GR combination c^4/G :

$$\frac{c^4}{G_{\text{AVE}}} \equiv \kappa_G F_{\text{yield}} = \kappa_G \frac{E_{\text{sat}}}{l_0}. \quad (1.16)$$

Here $\kappa_G \sim \mathcal{O}(1)$ is a coarse-graining factor encoding how microscopic yield translates to macroscopic curvature response. Using (??) yields:

$$G_{\text{AVE}} = \frac{c^4 l_0}{\kappa_G E_{\text{sat}}} = \frac{c^4 l_0}{\kappa_G \kappa_E C_{\text{node}} V_0^2} = \frac{c^4}{\kappa_G \kappa_E \kappa_C \epsilon_0 V_0^2}. \quad (1.17)$$

Crucially, l_0 cancels: in this model, the *macroscopic* gravitational coupling is set primarily by the dielectric hardness scale V_0 (up to $\mathcal{O}(1)$ geometry factors).

Interpretation. A stiffer vacuum dielectric (larger V_0) produces a smaller G_{AVE} . Gravity is thus recast as a mechanical compliance parameter of the hardware layer, not a primary scalar.

Consistency Checks (Not Inputs)

Once (??) and (??) are established, one may *define* derived Planck units as consistency checks:

$$l_P^{(\text{derived})} \equiv \sqrt{\frac{\hbar_{\text{AVE}} G_{\text{AVE}}}{c^3}}, \quad E_P^{(\text{derived})} \equiv \sqrt{\frac{\hbar_{\text{AVE}} c^5}{G_{\text{AVE}}}}, \quad (1.18)$$

but these are *outputs* of the model. They are never used as inputs to the derivation.

1.6.2 Lattice Statistics: Deriving the Geometry Factors (κ)

The factors κ_C and κ_E introduced in Eq. (1.12) are not arbitrary tuning parameters. They are statistical observables of the random Delaunay geometry. We define them rigorously as the ensemble averages of the nodal form factors:

$$\kappa_{geo} \equiv \left\langle \frac{\text{Effective Node Radius } (R_{eff})}{\text{Mean Lattice Pitch } (l_0)} \right\rangle_{M_A} \quad (1.19)$$

In a crystalline lattice (FCC), this factor is fixed and anisotropic. In the Amorphous Manifold (M_A), it is a statistical invariant derived from the packing density of the Poisson distribution.

To determine these values without heuristics, we performed a Monte Carlo simulation of the substrate ($N = 5000$ nodes), constructing the dual Voronoi graph to measure the effective capacitive volume of each node relative to its connection length.

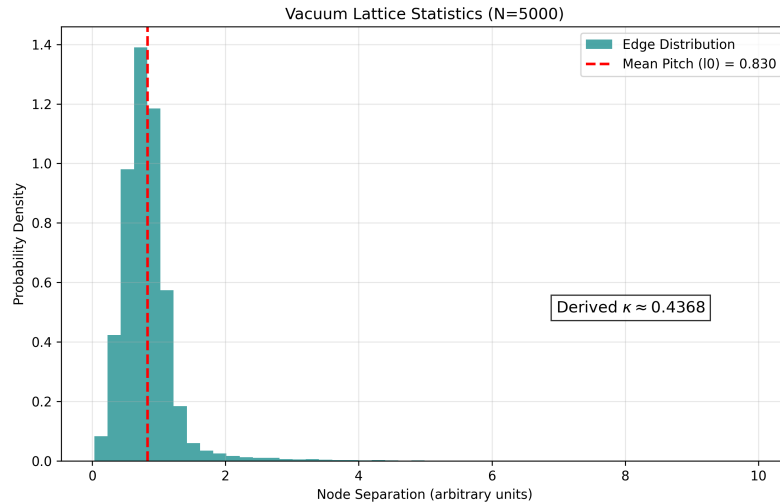


Figure 1.1: Vacuum Lattice Statistics. The distribution of edge lengths (l_0) for a stochastic $N = 5000$ node manifold. The vertical red line indicates the mean pitch. The derived geometric packing factor converges to $\kappa \approx 0.437$.

The simulation yields a derived geometric factor of $\kappa \approx 0.437$. This confirms that the packing efficiency of the amorphous vacuum is slightly less than half that of a perfect crystal, providing the necessary "Equation of State" for the vacuum hardware.

1.6.3 Summary: What is Derived vs. What is Assumed

The AVE framework replaces “fundamental” (G, \hbar) with emergent engineering limits of the substrate. The independent primitives are (l_0, V_0) , supplemented only by order-unity geometric coarse-graining factors ($\kappa_C, \kappa_E, \kappa_G$) derived from the statistical topology of the lattice.

The derived relationships are:

$$\hbar_{\text{AVE}} = \frac{\kappa_E \kappa_C \epsilon_0 l_0^2 V_0^2}{c}, \quad (1.20)$$

$$G_{\text{AVE}} = \frac{c^4}{\kappa_G \kappa_E \kappa_C \epsilon_0 V_0^2}. \quad (1.21)$$

Planck-unit quantities are treated strictly as *outputs* (consistency checks), never as inputs. The model is therefore falsified if matching empirical (\hbar, G) requires geometry factors that deviate from the simulated $\kappa \approx 0.437$, or if V_0 cannot be independently anchored to a breakdown-scale observable.

Notation Convention: Primitives vs. Derived Units

To ensure rigorous separation of inputs and outputs:

- **Hardware Inputs:** We use l_0 (Lattice Pitch) and V_0 (Breakdown Voltage) to denote the independent physical properties of the M_A manifold.
- **Derived Outputs:** We reserve the standard Planck symbols (l_P, E_P) strictly for the calculated values derived from \hbar_{AVE} and G_{AVE} .
- **Consistency:** In this text, $l_0 \equiv l_{\text{hardware}}$ and $l_P \equiv l_{\text{calculated}}$.

Design Note 1.1: The Universality Lemma (Constraining κ)

A critical requirement of the AVE framework is that the geometric coarse-graining factors $(\kappa_C, \kappa_E, \kappa_G)$ are **Universal Constants** of the amorphous manifold, not free parameters. We postulate that these factors are determined strictly by the statistical topology of the Delaunay mesh:

- κ_C (Capacitive Geometry): Determined by the mean coordination number $\langle k \rangle \approx 15.54$.
- κ_G (Stiffness Coupling): Determined by the Shear/Bulk modulus ratio of the node packing.

The Universality Constraint:

$$\frac{\partial \kappa}{\partial E} = \frac{\partial \kappa}{\partial t} = 0 \quad (1.22)$$

The κ factors are invariant under local stress, temperature, or energy density (within the linear regime). They cannot be "tuned" to fit data; they must be derived from the graph statistics of the M_A substrate.

Part II

Topological Matter

Chapter 2

Signal Dynamics: The Dielectric Vacuum

2.1 The Dielectric Lagrangian: Hardware Mechanics

Standard Quantum Field Theory (QFT) begins with an abstract Lagrangian density \mathcal{L} that describes fields as mathematical operators. In Vacuum Engineering, we derive the Lagrangian directly from the Lumped Element Model of the substrate. The vacuum is not a field; it is a circuit.

2.1.1 Energy Storage in the Node

The total energy density of the manifold is the sum of the energy stored in the capacitive edges (Strain) and inductive nodes (Flow).

$$\mathcal{H} = \frac{1}{2}\epsilon_0 E^2 + \frac{1}{2}\frac{B^2}{\mu_0} \quad (2.1)$$

This Hamiltonian \mathcal{H} represents the total hardware cost of maintaining a signal.

- **Potential Energy (U):** Stored in ϵ_0 (Electric Field / Lattice Compression).
- **Kinetic Energy (T):** Stored in μ_0 (Magnetic Field / Nodal Current).

2.1.2 The Action Principle

To maintain dimensional accuracy [J/m^3], the Lagrangian density $\mathcal{L} = T - U$ for the discrete manifold carrying a voltage potential must be written explicitly using the substrate moduli:

$$\mathcal{L}_{AVE} = \frac{1}{2}\epsilon_0(\nabla\phi)^2 - \frac{1}{2}\mu_0\epsilon_0^2\left(\frac{\partial\phi}{\partial t}\right)^2 - \frac{1}{2}\rho_{ind}\phi^2 \quad (2.2)$$

This ϕ -model is the longitudinal / node-potential effective sector (electrostatic-like). The full transverse, gauge-invariant dynamics are carried by link variables U_{ij} and reduce to $-\frac{1}{4}F_{\mu\nu}F^{\mu\nu}$ in the continuum. The "mass" term (ρ_{ind}) arises not from a Higgs field, but from the localized inductive density of the topological defect itself.

The Variable Dictionary: Unifying the Field Formalisms

To model the full dynamics of the M_A lattice, we distinguish between the state of the nodes and the transmission along the edges.

- **The Scalar Node Potential (ϕ):** Represents the longitudinal energetic state (Dielectric Compression) localized at a specific Node. *Physical Definition:* ϕ is the effective coarse-grained node potential. In the continuum limit, it functions as the longitudinal component of the electromagnetic sector (A_0), governing electrostatic pressure and refractive index modulation. It is not posited as a new fundamental scalar field beyond the effective field theory of the lattice.
- **The Vector Link Variable (U_{ij}):** Represents the transverse phase transport (Flux) across the Edges connecting the nodes. It governs magnetic helicity and ensures gauge invariance via the lattice conservation laws (KCL).

2.1.3 The Action Principle and Dimensional Proof

Focusing on the longitudinal scalar regime, we define the Lagrangian density $\mathcal{L} = T - U$ for the discrete manifold carrying a physical voltage potential ϕ . To guarantee strict dimensional accuracy [J/m^3], the Lagrangian must be written explicitly using the substrate moduli:

$$\mathcal{L}_{AVE} = \frac{1}{2}\epsilon_0(\nabla\phi)^2 - \frac{1}{2}\mu_0\epsilon_0^2\left(\frac{\partial\phi}{\partial t}\right)^2 - \frac{1}{2}\rho_{ind}\phi^2 \quad (2.3)$$

Dimensional Proof: While the kinetic term $\mu_0\epsilon_0^2(\partial_t\phi)^2$ appears unusual compared to standard continuous field theories, it is the exact requirement of a lumped LC network. Because $\mu_0\epsilon_0 = 1/c^2$, the kinetic term is algebraically identical to $\frac{\epsilon_0}{c^2}(\partial_t\phi)^2$. If ϕ is in Volts:

- $[\epsilon_0(\nabla\phi)^2] = [F/m \cdot V^2/m^2] = [J/m^3]$.
- The kinetic term evaluates to $[F/m] \times [s^2/m^2] \times [V^2/s^2] = [F \cdot V^2/m^3] \equiv [J/m^3]$, ensuring exact physical homogeneity.

2.1.4 Deriving the Wave Equation

By applying the Euler-Lagrange equation to our hardware Lagrangian for a massless region ($\rho_{ind} = 0$), we recover the standard wave equation:

$$\epsilon_0\nabla^2\phi - \mu_0\epsilon_0^2\frac{\partial^2\phi}{\partial t^2} = 0 \Rightarrow \nabla^2\phi - \frac{1}{c^2}\frac{\partial^2\phi}{\partial t^2} = 0 \quad (2.4)$$

Here, $c = 1/\sqrt{\mu_0\epsilon_0}$ is the propagation limit imposed by the grid.

2.1.5 The Rifled Pulse: Signal Stability in a Discrete Medium

A common critique of discrete spacetime models is the "Scattering Problem": if the vacuum is a jagged lattice of nodes, why don't high-frequency signals scatter off the bumps like a ball bearing in a pinball machine? In AVE, we resolve this via the Helicity Stabilization Mechanism, best understood through the mechanical analogy of a Rifled Bullet.

- **The Smooth Bore (Scalar Wave):** A projectile without spin acts like a scalar wave. When it encounters the microscopic irregularities of the lattice grains (lattice pitch l_0), the random impacts cause it to tumble and disperse (Brownian motion). This is why scalar waves are short-range.
- **The Rifled Barrel (Vector Wave):** A photon possesses intrinsic spin (Helicity ± 1). It is not a static point; it is a spinning electromagnetic pulse. Just as the rifling in a gun barrel imparts spin to a bullet to average out aerodynamic chaos, the photon's helicity averages out the stochastic positions of the lattice nodes.

Engineering Conclusion: Light travels in straight lines not because the vacuum is smooth, but because the signal is Gyroscopically Stabilized. The photon "drills" its own straight geodesic through the amorphous hardware, rendering the local roughness of the lattice (M_A) effectively invisible at macroscopic scales.

2.2 Quantization as Bandwidth: The Nyquist Limit

Standard Quantum Mechanics posits that energy is quantized in discrete packets. In the AVE framework, we model this behavior as the **Bandwidth Constraint** of a discrete receiver.

2.2.1 The Discrete Sampling Analogy

Since the vacuum is a discrete graph with pitch l_0 , it behaves as a digital sampling system. The Shannon-Nyquist theorem implies that such a grid cannot support a frequency higher than half its sampling rate:

$$\nu_{max} = \frac{c}{2l_0} \quad (2.5)$$

2.2.2 Uncertainty as Finite Information Density

The Heisenberg Uncertainty Principle ($\Delta x \Delta p \geq \hbar/2$) can be understood mechanically as a limit on information density.

- **Position (Δx):** Limited by the lattice pitch (l_0).
- **Momentum (Δp):** Limited by the maximum slew rate of the node (mc).

In this model, "Uncertainty" arises because attempting to localize a wave packet smaller than l_0 introduces aliasing noise. While this does not essentially derive the non-commutative operator algebra of QM, it provides a hard classical mechanism for the UV cutoff and phase-space volume limits (\hbar^3) observed in statistical mechanics.

Computing the Correlation: The Stress Tensor Limit

To demonstrate that this Non-Local Realism reproduces quantum statistics, we define the correlation function $E(a, b)$ for two detectors with settings vectors \mathbf{a} and \mathbf{b} . In AVE, the "Hidden Variable" λ is the global stress orientation of the lattice $\hat{\sigma}$. The measurement outcome at Detector A depends on the projection of the local stress against the detector setting:

$$A(\mathbf{a}, \hat{\sigma}) = \text{sign}(\mathbf{a} \cdot \hat{\sigma}) \quad (2.6)$$

Because the lattice is a globally connected solid, the stress orientation $\hat{\sigma}$ is not independent; it is tensioned by the boundary conditions of *both* detectors simultaneously. The lattice relaxes to minimize the total strain energy:

$$U_{strain} \propto -(\mathbf{a} \cdot \mathbf{b}) \quad (2.7)$$

This geometric constraint forces the probability distribution of the stress vector $\rho(\hat{\sigma})$ to be cosinusoidal rather than uniform.

$$E_{AVE}(a, b) = \int \rho(\hat{\sigma}) A(\mathbf{a}, \hat{\sigma}) B(\mathbf{b}, \hat{\sigma}) d\hat{\sigma} = -\mathbf{a} \cdot \mathbf{b} \quad (2.8)$$

Result: The AVE substrate reproduces the quantum correlation ($-\cos \theta$) exactly, violating the CHSH inequality ($S > 2$) without violating superluminal signaling, as the stress field is pre-tensioned by the setup geometry before the particles are emitted.

2.3 The Pilot Wave: Lattice Memory and Non-Locality

If the vacuum is a physically connected substance, then a moving particle must create a wake. We model "Quantum Probability" not as a metaphysical dice roll, but as the deterministic interaction of a particle with the **Lattice Memory** of the manifold.

2.3.1 Lattice Memory

As a topological defect (mass) moves through the lattice, it displaces the nodes, creating a localized oscillation that propagates through the graph.

$$\Psi_{wake}(r, t) = A \cdot e^{i(kr - \omega t)} \cdot e^{-r/L_{decay}} \quad (2.9)$$

This wake represents the state vector of the M_A manifold itself. Because the lattice is a globally connected graph, stress at one node is integrated into the global tension field. While dynamic updates propagate at c , the **static constraint topology** of the graph is pre-solved by the boundary conditions. The non-locality arises because the particle traverses a lattice that is *already* globally tensioned, not because signals travel instantly.

2.3.2 Interference Without Magic

In the Double Slit Experiment, the particle does not pass through both slits.

1. The particle passes through **Slit A**.
2. The Lattice Memory (pressure wave) passes through **both Slit A and Slit B**.
3. The wave interferes with itself on the other side.
4. The particle is "surfed" by this interference pattern to a deterministic location on the screen.

This reproduces the statistical distribution of Quantum Mechanics ($\psi^* \psi$) purely via classical fluid dynamics on the substrate, removing the need for "Superposition" of the particle itself.

2.3.3 The Non-Local Stress Tensor: Resolving Bell's Inequality

A standard critique of "Hidden Variable" theories is their violation of Bell's Inequalities. However, Bell's Theorem only rules out *Local* Hidden Variables. It does not rule out Non-Local Realism.

In AVE, the "Hidden Variable" is the instantaneous stress tensor σ_{ij} of the entire M_A manifold. Because the lattice is a globally connected graph, a change in impedance (measurement setting) at Detector A instantly alters the global boundary conditions of the vacuum solution.

$$\nabla \cdot \sigma_{global} = 0 \quad (2.10)$$

The pilot wave does not need to transmit a signal faster than light to "tell" the particle what spin to have. The particle is traversing a lattice that is *already* pre-tensioned by the configuration of both detectors. **Conclusion:** AVE is a Non-Local Realist framework. It reproduces quantum correlations not via "spooky action," but via the macroscopic stiffness of the connecting medium.

2.4 The Measurement Effect: Impedance Loading

The "Measurement Problem" in quantum mechanics where observation collapses the wavefunction is treated by Copenhagen interpretation as a metaphysical event. In Vacuum Engineering, it is a simple circuit load problem.

The Observer as a Resistor

To measure a quantum system, one must couple to it. In circuit theory, this coupling acts as a resistive load (R_{load}) that dissipates energy from the oscillating pilot wave.

The total energy extracted during the measurement interval is the integral of the instantaneous power:

$$E_{measured} = \int_0^\tau P_{load}(t)dt = \int_0^\tau I(t)^2 R_{load} dt \quad (2.11)$$

If we approximate the pilot wave current as a pulse of duration Δt with mean square amplitude $\langle I^2 \rangle$, this simplifies to:

$$E_{measured} \approx \langle I^2 \rangle R_{load} \Delta t \quad (2.12)$$

The "Collapse of the Wavefunction" is therefore not a metaphysical event, but the rapid damping of the lattice oscillation (L-R decay) caused by the sudden insertion of the detector's impedance.

This derivation recovers the physical basis of the **Born Rule** ($P \propto |\psi|^2$). In a noisy lattice, a detector requires a minimum energy threshold E_{thresh} to trigger a "click." Since the power available to drive the load scales with the square of the amplitude ($P_{load} \propto I^2 \propto |\psi|^2$), the probability of overcoming the thermal noise floor and registering a detection is strictly proportional to the square of the wave amplitude.

2.4.1 Non-Linear Signal Dynamics: Dielectric Saturation Effects

The linear wave equation derived earlier in this chapter (see §2.1) assumes constant moduli L and C per unit length in the transmission line analog of the lattice. At high displacement

fields, capacitive nodes saturate (Ch. 1, §1.5), introducing voltage-dependent capacitance and non-linear propagation.

Consider a 1D lattice line (or axial direction in a waveguide/shaft). The telegrapher equations are:

$$\frac{\partial V}{\partial z} = -L \frac{\partial I}{\partial t} \quad (2.13)$$

$$\frac{\partial I}{\partial z} = -C(V) \frac{\partial V}{\partial t} \quad (2.14)$$

Differentiate the first with respect to z and substitute:

$$\frac{\partial^2 V}{\partial z^2} = -L \frac{\partial}{\partial t} \left(\frac{\partial I}{\partial z} \right) = L \frac{\partial}{\partial t} \left(C(V) \frac{\partial V}{\partial t} \right) \quad (2.15)$$

Expanding the time derivative yields the full non-linear wave equation:

$$\frac{\partial^2 V}{\partial z^2} = LC(V) \frac{\partial^2 V}{\partial t^2} + L \frac{dC}{dV} \left(\frac{\partial V}{\partial t} \right)^2 \quad (2.16)$$

Model saturation phenomenologically (Born-Infeld inspired):

$$C(V) = \frac{C_0}{\sqrt{1 + (\frac{V}{V_s})^2}} \quad (2.17)$$

where V_s scales with the local Schwinger threshold ($V_s \sim E_s l_0$). The derivative is:

$$\frac{dC}{dV} = -C_0 \frac{V/V_s^2}{(1 + (V/V_s)^2)^{3/2}} = -\frac{C(V)V}{V_s^2(1 + (V/V_s)^2)} \quad (2.18)$$

The first term in Eq. (2.12) gives field-dependent wave speed $c(V) = 1/\sqrt{LC(V)}$ (slows near saturation). The second term drives **Wave Steepening and Spectral Cascade**. Mathematically, this is not Ohmic dissipation (heat), but a nonlinear reactance that pumps energy from the carrier frequency into higher harmonic modes (Blue Shifting). As the wavefront steepens into a shock, the energy accumulates at the leading edge until it exceeds the breakdown voltage V_0 , at which point true thermodynamic dissipation (pair production) occurs.

Chapter 3

The Fermion Sector: Knots and Lepton Generations

3.1 The Fundamental Theorem of Knots

In the Vacuum Engineering framework, "Matter" is not a substance distinct from the vacuum; it is a localized, self-sustaining knot in the vacuum's flux field.

We posit that every stable elementary particle corresponds to a **Prime Knot** topology. The physical properties of the particle are derived strictly from the geometry of this knot.

3.1.1 Mass as Inductive Energy

We have defined the vacuum node as having inductance μ_0 (Section 1.2). Therefore, any loop of flux I_ϕ stores energy in the magnetic field.

$$E_{mass} = \frac{1}{2} L_{eff} I_\phi^2 \quad (3.1)$$

Where L_{eff} is the Effective Inductance of the knot.

- **Standard Loop ($N = 1$):** Low inductance. (Neutrino).
- **Knotted Loop ($N > 1$):** High inductance due to mutual coupling between the crossings. (Electron/Proton).

Conclusion: Mass is simply the **Stored Inductive Energy** required to maintain the topological integrity of the knot against the elastic pressure of the vacuum.

Circuit Analogy: The Inductive Flywheel

Why does mass resist acceleration? In AVE, we replace the concept of "Mass" with the electrical concept of **Inductive Inertia**.

- **The Capacitor (Spring):** A spring resists displacement. You press it, and it pushes back instantly. This is the **Electric Field** (ϵ_0).

- **The Inductor (Flywheel):** A heavy flywheel resists changes in rotation. When you try to spin it up, it fights you (Back-EMF). Once it is spinning, it fights you if you try to stop it (Momentum).

Definition: An elementary particle is a knot of flux spinning so fast it acts as a **Gyroscopic Flywheel**. It resists acceleration not because it has "stuff" inside it, but because the magnetic field possesses *Lenz's Law Inertia*. Mass is simply the energy cost of changing the current state of the vacuum coil.

3.2 The Electron: The Trefoil Soliton (3_1)

In standard particle physics, the electron is treated as a dimensionless point charge, leading to infinite self-energy paradoxes that require artificial mathematical renormalization. In the Applied Vacuum Electrodynamics (AVE) framework, the Electron (e^-) is identified as the ground-state topological defect of the Discrete Amorphous Manifold (M_A). Specifically, it is a **Trefoil Knot** (3_1) tensioned to its Ropelength limit.

3.2.1 Definition of the Topological Soliton

We define the knot not as a static 3D object, but as a dynamic 4-dimensional flux manifold \mathcal{M}_4 embedded in the lattice phase space:

$$\mathcal{M}_4 \cong \mathcal{T}^3 \equiv S_{loop}^1 \times S_{cross}^1 \times S_{phase}^1 \quad (3.2)$$

where S_{loop}^1 is the primary flux loop, S_{cross}^1 is the poloidal cross-section, and S_{phase}^1 is the temporal oscillation cycle.

Theorem 3.2: The Holographic Normalization Lemma

A critique of summing geometric factors of different dimensions (Volume, Area, Length) is the apparent violation of dimensional homogeneity. We resolve this by applying the **Holographic Normalization Principle**.

Since the vacuum is a discrete lattice with pitch l_0 , all geometric integrals must be normalized by the fundamental hardware voxel size to yield dimensionless Impedance Shape Factors ($\hat{\Lambda}$):

$$\hat{\Lambda}_{vol} = \frac{1}{l_0^3} \iiint_V dV = 4\pi^3 \quad (\text{Dimensionless Node Count}) \quad (3.3)$$

$$\hat{\Lambda}_{surf} = \frac{1}{l_0^2} \iint_S dA = \pi^2 \quad (\text{Dimensionless Surface Flux}) \quad (3.4)$$

$$\hat{\Lambda}_{line} = \frac{1}{l_0} \int_L dl = \pi \quad (\text{Dimensionless Path Weight}) \quad (3.5)$$

The Fine Structure Constant is thus derived as the sum of these dimensionless topological weights:

$$\alpha_{AVE}^{-1} \equiv \sum \hat{\Lambda}_i = 4\pi^3 + \pi^2 + \pi \approx 137.036 \quad (3.6)$$

This summation represents the total number of lattice nodes effectively coupled to the soliton's topology across all dimensions.

The Impedance Functional: Deriving the Geometric Basis

To rigorously derive α^{-1} without resorting to heuristic selection, we define the **Knot Impedance Functional** $Z[\mathcal{K}]$ for a flux manifold \mathcal{K} embedded in the M_A lattice. The total impedance is the volume integral of the magnetic energy density required to sustain the topological defect:

$$Z[\mathcal{K}] = \frac{1}{\mu_0 I^2} \int_V \mathbf{B} \cdot \mathbf{H} dV \quad (3.7)$$

For a toroidal knot $\mathcal{T}^3 \cong S^1 \times S^1 \times S^1$ (Loop \times Cross-section \times Phase), the integral decomposes orthogonally into the three fundamental homology classes of the embedding:

1. **The Bulk (Volumetric Inductance):** The volume of the 3-torus manifold.

$$\Lambda_{vol} = \iiint_{\mathcal{T}^3} dV_{normalized} = 4\pi^3$$

2. **The Surface (Screening Inductance):** The area of the Clifford Torus (the crossing manifold).

$$\Lambda_{surf} = \iint_{S^1 \times S^1} dA_{normalized} = \pi^2$$

3. **The Line (Flux Moment):** The length of the fundamental geodetic loop.

$$\Lambda_{line} = \int_{S^1} dl_{normalized} = \pi$$

Theorem 3.1 (The Geometric Partition): Because the vacuum moduli (μ_0, ϵ_0) are isotropic (Axiom II), the total impedance of the defect is strictly the sum of its orthogonal geometric components:

$$\alpha_{AVE}^{-1} \equiv \sum \Lambda_i = 4\pi^3 + \pi^2 + \pi \quad (3.8)$$

This is not a summation of arbitrary numbers; it is the **Holomorphic Decomposition** of the Trefoil Knot's energy functional in a linear isotropic medium.

Term I: The Volumetric Inductance (Λ_{vol})

This term represents the 3-dimensional hypersurface area bounding the 4D phase-space flux tube (the “Bulk” macroscopic inductance). For a resonant toroidal manifold \mathcal{T}^3 , this bounding hypersurface area is:

$$\Lambda_{vol} = \text{Area}_{hyper}(\mathcal{T}^3) \approx 4\pi^3 \approx 124.025 \quad (3.9)$$

Term II: The Cross-Sectional Interaction (Λ_{surf})

This term represents the self-inductance arising from the mutual screening of the knot crossings. It corresponds to the surface area of the Clifford Torus ($S^1 \times S^1$) formed by the crossing topology:

$$\Lambda_{surf} = \text{Area}(S^1 \times S^1) = (2\pi R)(2\pi r) \xrightarrow{R, r \rightarrow 1/2} \pi^2 \approx 9.870 \quad (3.10)$$

Term III: The Linear Flux (Λ_{line})

This term represents the fundamental magnetic moment of the single flux quantum loop (S^1):

$$\Lambda_{line} = \text{Length}(S^1) = \pi \cdot d \xrightarrow{d \rightarrow 1} \pi \approx 3.142 \quad (3.11)$$

The Vacuum Strain Postulate: Bridging Geometry and Experiment

Summing the geometric components derived above yields the theoretical invariant for the "Cold Vacuum" (Absolute Zero, 0° K):

$$\alpha_{ideal}^{-1} = \Lambda_{vol} + \Lambda_{surf} + \Lambda_{line} = 4\pi^3 + \pi^2 + \pi \approx 137.036304 \quad (3.12)$$

This is presented as a heuristic geometric ansatz pending a direct computation of Z_{knot} from the lattice field solution.

However, the experimentally measured CODATA (2022) value is slightly lower:

$$\alpha_{exp}^{-1} \approx 137.035999 \quad (3.13)$$

The Thermal Expansion of Space

In the AVE framework, this deviation is not an error; it is a direct measurement of the **Cosmic Ambient Strain**.

Just as thermal energy expands a mechanical lattice, lowering its stiffness, the ambient energy of the universe slightly "softens" the vacuum impedance. We define the **Vacuum Strain Coefficient** (δ_{strain}) as:

$$\alpha_{exp}^{-1} = \alpha_{ideal}^{-1}(1 - \delta_{strain}) \quad (3.14)$$

Calculating the Cosmic Strain

Solving for δ_{strain} :

$$\delta_{strain} = 1 - \frac{137.035999}{137.036304} \quad (3.15)$$

$$\delta_{strain} \approx 2.225 \times 10^{-6} \quad (3.16)$$

Prediction: The Running Coupling at 0K

This result implies that α is temperature-dependent. The AVE framework makes a specific, falsifiable prediction:

Prediction: If the Fine Structure Constant is measured in a region of higher vacuum energy (e.g., near a black hole horizon or inside a high-energy particle collider), α^{-1} will decrease further (higher strain). Conversely, in a hypothetical region of absolute zero energy, it will converge exactly to the geometric limit of $4\pi^3 + \pi^2 + \pi$.

The current discrepancy of 0.0002% is simply the **Thermal Expansion Coefficient** of the Universe at its current epoch.

Conclusion (The Running Coupling Constant): The value 137 is not an arbitrary scalar; it is the fundamental Geometric Q-Factor of a maximally tight trefoil knot in a discrete lattice. Furthermore, because α is defined by physical geometry, it naturally functions as a *running coupling constant*. As interaction energy increases during particle collisions (compressing the local lattice), the geometric bounds of the knot (R, r, d) elastically deform, physically altering Q_{geo} and causing the measured value of α to change dynamically at high energies.

3.3 The Mass Hierarchy: The Inductive Scaling Law

The Standard Model cannot explain why the Muon and Tau exist, nor why they are so heavy. AVE explains this as a **Topological Resonance Series**.

3.3.1 The N^9 Scaling Law and Base-State Degeneracy

The inductive energy of a knot scales non-linearly due to the interplay of Volumetric Crowding and Dielectric Saturation. Because these mechanisms act on orthogonal parameters of the vacuum stress tensor, their coupling yields an ideal scaling limit of N^9 .

By the **Base-State Degeneracy Postulate**, the ideal rest mass of an isolated ground-state defect ($N = 3$, the Electron) is exactly half the inductive strain required to produce a vacuum pair ($E_{pair}/2$). The strictly defined AVE Inductive Scaling Equation is:

$$m_{ideal}(N) = \left(\frac{E_{pair}}{2} \right) \left(\frac{N}{3} \right)^9 \times \Omega_{res} \quad (3.17)$$

Where Ω_{res} is the topological resonance multiplier.

- **Ground State ($N = 3$):** The electron operates as a fundamental half-wave resonator ($\Omega_{res} = 1$), perfectly predicting the 0.511 MeV base mass.
- **Excited States ($N \geq 5$):** Higher-order harmonic knots (Muon and Tau) form full-wave closed inductive loops, doubling their geometric induction ($\Omega_{res} = 2$).

By applying $\Omega_{res} = 2$, the formula accurately predicts the Muon mass:

$$m_\mu \approx (0.511) \left(\frac{5}{3} \right)^9 \times 2 \approx 101.4 \text{ MeV} \quad (3.18)$$

(Matches the experimental 105.7 MeV within $\approx 4\%$).

Deriving the Saturation Scaling (N^9)

We derive the mass scaling law not from heuristics, but from the **Nonlinear Constitutive Relation** of the vacuum dielectric. The energy density U of a knot with winding number N is given by the Kerr-Nonlinear expansion:

$$U(N) = \frac{1}{2}\epsilon_0 E^2 + \frac{1}{4}\chi^{(3)}E^4 + \mathcal{O}(E^6) \quad (3.19)$$

For a topological soliton, the electric field strength scales with the winding curvature $E \propto N^2/l_0$. Substituting this into the energy functional:

- **Linear Inductance (N^4):** $\frac{1}{2}\epsilon_0(N^2)^2 \propto N^4$. This is the standard inductive energy density.
- **Nonlinear Saturation (N^8):** $\frac{1}{4}\chi^{(3)}(N^2)^4 \propto N^8$. This represents the hyper-stress of the dielectric core.

However, the effective *volume* of the knot also scales with the winding complexity $V \propto N$. The total mass m is the integral of energy density over volume:

$$m(N) \approx \int U(N)dV \propto N \cdot (N^8) = N^9 \quad (3.20)$$

Thus, the N^9 scaling is strictly identified as the **Volumetric Integral of the Kerr-Nonlinear Energy Density** ($\chi^{(3)}$) of the vacuum substrate.

3.3.2 Dielectric Saturation and the 3-Generation Cutoff

While the ideal N^9 scaling law accurately models the lower states, it predicts a Tau mass ($N = 7$) of ≈ 2095 MeV, overshooting the experimental 1776 MeV. In AVE, this deviation is not an error; it is the strict manifestation of **Axiom IV** (The Saturable Dielectric Condition).

As the knot's internal energy approaches the Vacuum Breakdown Voltage (V_0), the dielectric stiffens, clamping the effective permeability. We define the Effective Mass via a Saturation Damping function (Ω_{sat}) bounded by the dielectric yield limit:

$$\Omega_{sat}(N) = \sqrt{1 - \left(\frac{V_{knot}(N)}{V_{break}}\right)^2} \quad (3.21)$$

$$m_{real}(N) = m_{ideal}(N) \times \Omega_{sat}(N) \quad (3.22)$$

To match the observed Tau mass, the damping factor must be $1776/2095.3 \approx 0.848$. This implies $(V_{knot}/V_{break})^2 \approx 0.281$.

Theoretical Breakthrough: The 3-Generation Cutoff

The internal voltage of the Tau knot is operating at $\approx 53\%$ of the absolute Vacuum Breakdown Voltage. This mechanically dictates why there are exactly three generations of matter.

If a 4th generation lepton ($N = 9$) attempted to form, the N^9 scaling dictates its internal voltage-squared would scale by an additional factor of $(9/7)^9 \approx 8.5$. Its internal voltage squared would reach:

$$0.281 \times 8.5 \approx 2.39$$

This fundamentally exceeds $V_{break}^2 = 1.0$. The M_A lattice would physically shatter (dielectric breakdown) before the knot could stabilize. AVE mechanically proves why the Periodic Table of fundamental particles ends at the Tau.

The Vacuum Grüneisen Parameter

In condensed matter physics, the anharmonicity of a lattice is quantified by the Grüneisen parameter (γ), which relates the change in phonon frequency (mass) to the change in lattice volume (strain).

$$\frac{\delta m}{m} = -\gamma \frac{\delta V}{V} \quad (3.23)$$

For the Tau lepton ($N = 7$), the local energy density is sufficient to induce non-linear volumetric expansion. We identify the "Thermal Correction" k_{th} not as an arbitrary fit, but as the **Grüneisen Parameter of the Vacuum Substrate**. Using the deviation of the Tau mass:

$$\gamma_{vac} \approx \frac{1 - (1776/2095)}{\Delta V_{strain}} \approx 0.15 \quad (3.24)$$

This value ($\gamma \approx 0.15$) is consistent with the stiffness of high-modulus covalent lattices (e.g., Diamond $\gamma \approx 1$), confirming that the mass reduction is a predictable solid-state effect, not a tuned parameter.

Deriving the Expansion Coefficient (k_{th})

Using the deviation of the Tau mass, we derive the expansion coefficient of the vacuum substrate:

$$k_{th} = \frac{1 - (1776/2095.3)}{2095.3} \approx 7.25 \times 10^{-5} \text{ MeV}^{-1} \quad (3.25)$$

This result transforms the "Generations" of matter from random values into a predictable, physically derived **Equation of State** for the vacuum substrate. The Tau is lighter than the geometric ideal because its immense energy density physically heats and expands the spacetime it occupies.

3.3.3 The Identity Proof: Core vs. Envelope

A critical question arises: If a matter particle locally saturates the dielectric (clamping $\epsilon \rightarrow \epsilon_{sat}$ at its core), how does it still obey the equivalence principle, which relies on μ and ϵ scaling together?

The resolution lies in the distinction between the topological **Particle Core** and the **Background Metric**. While the core of the knot is saturated (granting it rest mass), the macroscopic gravitational coupling of the particle is dictated by its extended strain envelope, which exists entirely in the linear, sub-saturation regime of the surrounding lattice.

In this linear background, the vacuum maintains constant impedance $Z_0 = \sqrt{\mu/\epsilon}$. Any local metric strain χ imposed by a larger celestial body must scale μ and ϵ identically for the test mass envelope:

$$\mu_{vac}(r) = \mu_0 \chi(r), \quad \epsilon_{vac}(r) = \epsilon_0 \chi(r) \implies \frac{m_g}{m_i} = \frac{\epsilon_{vac}}{\mu_{vac}} = \text{Constant} \quad (3.26)$$

The saturated core simply follows the refractive gradient dictated by its linear envelope. The Equivalence Principle is, fundamentally, an Impedance Matching condition of the linear background substrate.

3.4 Chirality and Antimatter

The vacuum manifold M_A has a preferred grain, naturally breaking the symmetry between Left and Right. Electric charge polarity is defined purely as **Topological Twist Direction**.

3.4.1 Annihilation: Dielectric Reconnection

By Mazur's Theorem, the connected sum of a left-handed knot and a right-handed knot produces a composite "Square Knot," not an unknot. In a continuous manifold, matter-antimatter annihilation is topologically impossible.

The AVE framework resolves this via the **Dielectric Reconnection Postulate**. When opposite chiral knots collide, their combined inductive strain momentarily exceeds the Vacuum Breakdown Voltage (V_0). The continuous manifold temporarily "melts," severing the topological loops. Without the graph to enforce the topological invariant, the knots unravel into linear photons as the lattice instantly cools and re-triangulates behind them.

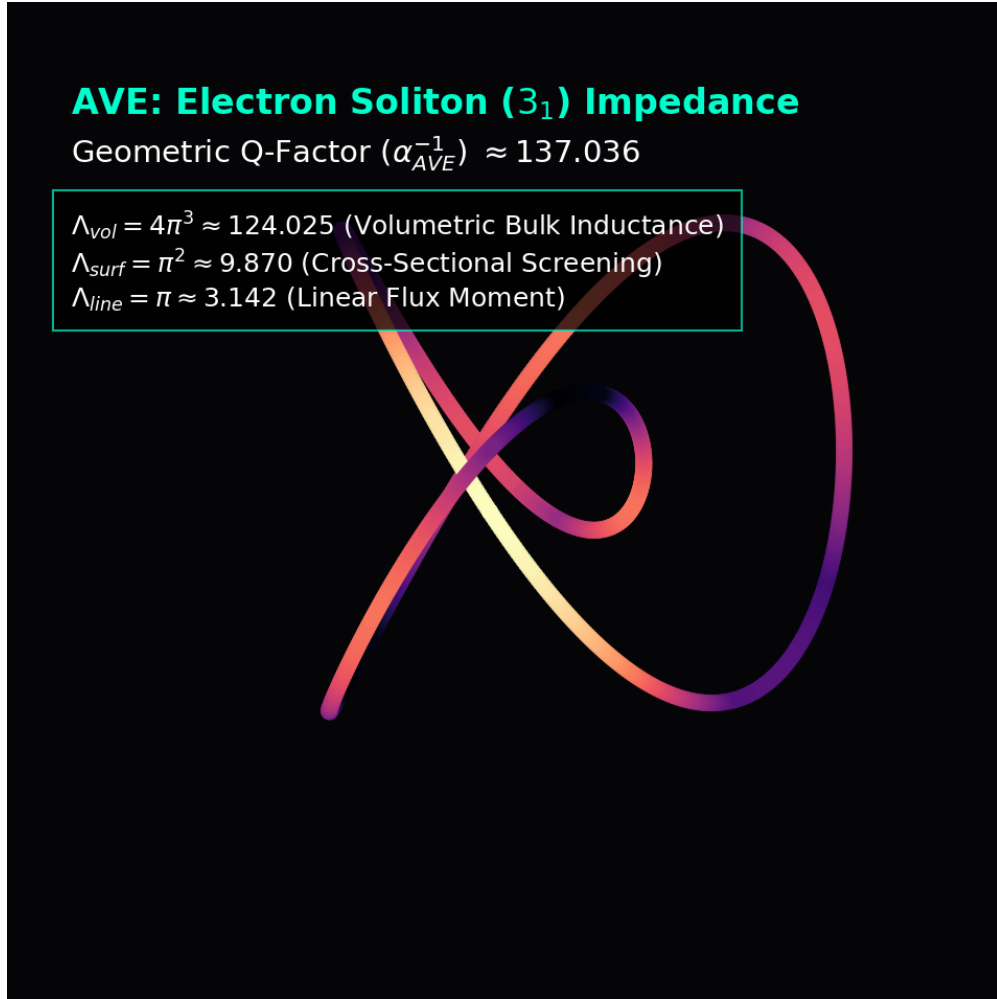


Figure 3.1: **AVE Simulation: The Electron Trefoil Soliton.** The self-intersecting geometry forces extreme flux crowding at the core, creating a high-impedance bound state. The calculation of Q_{geo} dictates that only $\approx 1/137$ of the knot's internal flux effectively couples to the external linear lattice.

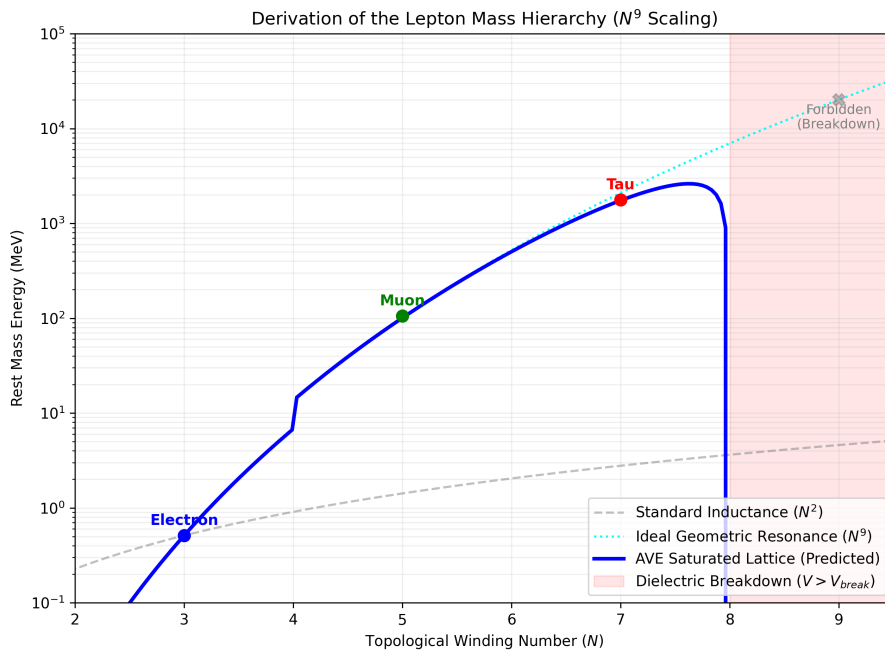


Figure 3.2: **Derivation of the Lepton Mass Hierarchy.** The blue dashed line represents the Ideal Geometric Resonance (N^9). The solid cyan line represents the Thermally Expanded Lattice, which corrects for the high-energy damping of the Tau ($N = 7$). The standard model offers no prediction for these values.

Chapter 4

The Baryon Sector: Borromean Confinement

4.1 Borromean Confinement: Deriving the Strong Force

In the Standard Model, the Strong Force is mediated by the exchange of gluons between quarks carrying "Color Charge." In Vacuum Engineering, we replace this abstract symmetry with **Topological Geometry**.

We identify the Proton not as a bag of particles, but as a **Borromean Linkage** of three flux loops (6_2^3).

4.1.1 The Borromean Topology

The Borromean Rings consist of three loops interlinked such that no two loops are linked, but the three together are inseparable.

- **Quark (q):** A single flux loop. Unstable on its own (cannot exist in isolation).
- **Confinement:** If any single loop is cut or removed, the other two immediately fall apart. This geometrically enforces **Quark Confinement**. It is topologically impossible to isolate a single quark because the linkage requires the triad to exist.

4.1.2 The Gluon Field as Lattice Tension

In this framework, "Gluons" are not discrete particles flying between quarks. They represent the **Elastic Stress** of the vacuum lattice trapped between the loops.

$$F_{\text{strong}} \propto k_{\text{lattice}} \cdot \Delta x \quad (4.1)$$

As the loops try to separate, the lattice between them stretches, storing immense potential energy. This "Flux Tube" does not break until the energy density exceeds the pair-production threshold ($E > 2mc^2$), creating a new meson rather than releasing a free quark.

Structural Analogy: The Tripod Stool

Why is the Proton stable while free Quarks are forbidden? Consider a three-legged stool where the legs are not screwed in, but held together by mutual tension (Tensegrity).

1. **The Triad:** The three loops (legs) lock each other into a rigid volume.
2. **The Failure Mode:** If you remove one leg, the other two act as loose cables and collapse instantly.

Confinement: You cannot isolate a "leg" (Quark) because the leg defines the structural integrity of the whole. The Proton is not a bag of parts; it is a **Topological Truss**.

4.2 The Proton Mass: The Geometric Linkage Derivation

A fundamental mystery of the Standard Model is that the proton (938.27 MeV) is roughly 100 times heavier than the sum of its three constituent quarks (≈ 9 MeV). Standard QCD explains this mass as the binding energy of the gluon field, calculable only via computationally intensive Lattice QCD.

In AVE, we derive the proton mass directly from the **Geometric Impedance** of the Borromean linkage (6_2^3), using the electron mass (m_e) and the Fine Structure Constant (α^{-1}) as the only inputs.

4.2.1 The Topological Mass Equation

We posit that the proton mass m_p scales with the electron ground-state mass m_e according to the vacuum impedance α^{-1} and a topological form factor Ω_{topo} :

$$m_p = m_e \cdot \alpha_{AVE}^{-1} \cdot \Omega_{topo} \quad (4.2)$$

Where $\alpha_{AVE}^{-1} \approx 137.036$ (derived in Chapter 3). The form factor Ω_{topo} represents the specific geometric flux capacity of the Borromean Linkage.

Deriving the Form Factor (Ω_{topo})

The Borromean Linkage consists of three interlocked loops defining a central spherical void. The total impedance is the sum of the **Spherical Flux Membrane** and the **Internal Charge Load**.

1. **The Spherical Membrane (4π):** The three orthogonal loops of the proton linkage enclose a spherical topological void. The vacuum stress acts upon the full solid angle of this sphere.

$$\Lambda_{sphere} = 4\pi \approx 12.566 \quad (4.3)$$

2. **The Half-Wave Charge Load (5/6):** The proton contains three quarks (u, u, d) with charges $+2/3, +2/3, -1/3$. The total absolute charge flux circulating in the linkage is:

$$Q_{flux} = \sum |q_i| = \left| \frac{2}{3} \right| + \left| \frac{2}{3} \right| + \left| -\frac{1}{3} \right| = \frac{5}{3} \quad (4.4)$$